REPORT DOCUMENTATION PAGE

AFRL-SR-AR-TR-05-

$0\,008$

1. REPORT DATE (DD-MM-YYYY)	2. REPORT TYPE	3. DATES COVERED (From - To)
	Final	15 Sep 2003 - 14 Sep 2004

4. TITLE AND SUBTITLE	5a. CONTRACT NUMBER
Selected Electromagnetic Problems in Electroencephalography (EEG), Fields in Complex Media, and Small Radiating Elements in Dissipative Media	
	5b. GRANT NUMBER
	F49620-03-1-0438
	5c. PROGRAM ELEMENT NUMBER

6. AUTHOR(S)	5d. PROJECT NUMBER
Nader Engheta	
Edward N. Pugh Jr.	5e. TASK NUMBER
	5f. WORK UNIT NUMBER

7. PERFORMING ORGANIZATION NAME(S) AND ADDRESS(ES)	8. PERFORMING ORGANIZATION REPORT NUMBER
The University of Pennsylvania Department of Electrical & Systems Engineering Philadelphia, PA 19104	

9. SPONSORING/MONITORING AGENCY NAME(S) AND ADDRESS(ES)	10. SPONSOR/MONITOR'S ACRONYM(S)
Air Force Office of Scientific Research 4015 Wilson Blvd Mail Room 713 Arlington, VA 22203	AFOSR
	11. SPONSOR/MONITOR'S REPORT NUMBER(S)

12. DISTRIBUTION/AVAILABILITY STATEMENT

Distribution Statement A. Approved for public release; distribution is unlimited.

13. SUPPLEMENTARY NOTES

14. ABSTRACT

From the electromagnetic point of view we can think of the brain as an inhomogeneous, lossy dielectric body, with complex geometry. The electrical activity of the brain is represented by the currents flowing inside it that is caused by the neuronal activities. We are interested in the electromagnetic modeling and analysis of the effects of those currents on the potential that can be measured on the scalp by MEG sensors. In order to have a qualitative understanding it's possible to use simplified models either for the whole brain or of some specific part of it.

15. SUBJECT TERMS

16. SECURITY CLASSIFICATION OF:			17. LIMITATION OF ABSTRACT	18. NUMBER OF PAGES	19a. NAME OF RESPONSIBLE PERSON
a. REPORT	b. ABSTRACT	c. THIS PAGE			Nader Engheta
U	U	U	UU		19b. TELEPHONE NUMBER (Include area code)

Standard Form 298 (Rev. 8/98)
Prescribed by ANSI Std. Z39.18

Final Report on

Grant Number F49PRE-03-1-0438

On the project entitled

Selected Electromagnetic Problems in Electroencephalography (EEG), Fields in Complex Media, and Small Radiating Elements in Dissipative Media

Duration: September 15, 2003-September 14, 2004

Principal Investigator:

Nader Engheta
University of Pennsylvania
Department of Electrical and Systems Engineering
Philadelphia, PA 19104
Tel: 215-898-9777
Fax: 215-573-2068
E-mail: engheta@ee.upenn.edu

Co-PI: Edward N. Pugh, Jr.
F. M. Kirby Center for Molecular Ophthalmology
University of Pennsylvania

Submitted to

Air Force Office of Scientific Research (AFOSR)
Dr. Arje Nachman and Dr. Richard Albanese
AFOSR/NM
4015 Wilson Blvd
Mail Room 713
Arlington, VA 22203

November 2004

20050112 010

Part 1: Some Electromagnetic Problems Relevant to the EEG Paradigm

Motivation and Background

It is well known that living tissues generate electrical activities. The electrical signals produced by the heart, known as the electrocardiogram, the ones generated by muscles, called electromyogram, and the one by the retina, named electroretinogram, have been studied by physicians, neuroscientists[1],[2],[3], and medical researchers. The brain also produces electrical activity, and the study of such activity, i.e., electroencephalography (EEG), has been the subject of research for neuroscientists, medical researchers and clinicians.[4],[5] Since these electrical signals are due to the stimulus-induced potentials and currents in the brain tissues, understanding and analyzing the electromagnetic characteristics of the potential and currents in inhomogeneous dissipative media becomes of paramount importance. We have studied and analyzed some selected electromagnetic problems that relate to the EEG paradigm.

(1) Electromagnetic model for the interpretation of the potential distribution over the scalp due to electrical activity inside the brain: Quasi-Static Approach

From the electromagnetic point of view we can think of the brain as an inhomogeneous, lossy dielectric body, with complex geometry. The electrical activity of the brain is represented by the currents flowing inside it that is caused by the neuronal activities. We are interested in the electromagnetic modeling and analysis of the effects of those currents on the potential that can be measured on the scalp by EEG sensors. In order to have a qualitative understanding it's possible to use simplified models either for the whole brain or of some specific part of it. A simplified model of the brain, effective as far as the potential distribution over the scalp is concerned, is well known multi-shelled (i.e., multilayered dielectric) sphere as depicted in the Figure 1. In this way, the shape of the brain is approximated by a three-shell spherical volume with the different complex permittivities in the various layers[4].

[1] A. L. Lyubarsky, and E. N. Pugh, Jr., "The recovery phase of the murine rod photoresponse reconstructed from electroretinographic recordings" *Journal of Neuroscience*, vol. 16, No. 2, pp. 563-571, 1996.

[2] A. L. Lyubarsky, B. Falsini, M. E. Pennesi, P. Valentini, and E. N. Pugh, Jr., "UV- and midwave-sensitive cone-driven retinal responses of the mouse: a possible phenotype for co-expression of cone photopigments", *Journal of Neuroscience* vol. 19, No. 1, pp. 442-455, 1999.

[3] E. N. Pugh, Jr., B. Falsini, and A. L. Lyubarsky, (1998) "The origin of the major rod- and cone-driven components of the rodent electroretinogram, and the effect of age and light-rearing history on the magnitudes of these components". In T.P. Williams and A.B. Thistle (Eds.), *Photostasis and Related Topics*, pp. 93-128. New York: Plenum, 1998.

[4] Paul. L. Nunez, *Electric Fields of the Brain: The Neurophysics of EEG*, Oxford University Press, 1981.

[5] David Regan, *Human Brain Electrophysiology: Evoked Potentials and Evoked Magnetic Fields in Science and Medicine*. Elsevier, New York, 1989.
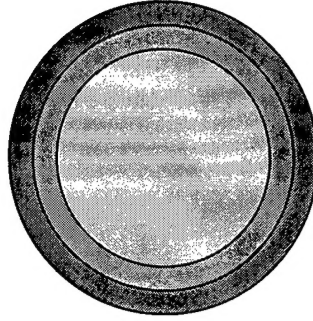
Figure 1 : Three-shell model of the brain

The structure depicted in Figure 1 may be analyzed either from the electrostatic or the electrodynamic point of view. Since the frequencies involved are very low, we can first consider the quasi-statis approach. .

In this model the three regions represent brain, skull and scalp and the whole structure is surrounded by unbounded free space. Each region has a different conductivity, and the surrounding medium has zero conductivity. We use this model to estimate the potential in each of the three regions and outside, due to the current sources located at a point inside the brain. We want to estimate the potential distribution in the structure, related to different configurations of the sources. The electrostatic problem to solve is the one of a current source inside a dissipative medium. From the continuity of charge, we have

$$\nabla \cdot \mathbf{J} = -\frac{\partial \rho}{\partial t} \tag{1}$$

In the quasi-static case, (1)is equal to:

$$\nabla \cdot \mathbf{J} \ \Box \ 0 \tag{2}$$

Furthermore, we assume that the Ohm law is applicable in our medium, so we can express the current density as the sum of an impressed current and a homic current:

$$\mathbf{J} = \mathbf{J}_{imp} + \sigma \mathbf{E} \tag{3}$$

where σ is the conductivity of the medium. For a "Point Source" we mean a point from which an impressed current flows into our medium. We will call a "negative source" a current sink. If we substitute (3) in the equation (2) we obtain:

$$-\nabla \cdot \sigma \mathbf{E} = \nabla \cdot \mathbf{J}_{imp} \tag{4}$$

In the quasi-static approximation, the electric field may be expressed as the negative gradient of a scalar potential:

$$\mathbf{E} = -\nabla \Psi \tag{5}$$

So we have:

$$\nabla \cdot \sigma \nabla \Psi = \nabla \cdot \mathbf{J}_{imp} \qquad (6)$$

Equation (6) has the same form of the Poisson equation:

$$\nabla \cdot \varepsilon \nabla \Psi = \rho \quad . \qquad (7)$$

Equation (7) is identical to equation (6) if we replace ε by σ and ρ by $\nabla \cdot \mathbf{J}_{imp}$, so as pointed out by Ref [4], we have only to solve a standard electrostatic problem and then make the substitution. For the case of a point source of current in a homogeneous medium with conductivity σ we have:

$$\Psi(r) = \frac{1}{4\pi\sigma} \frac{I}{r} \qquad (8)$$

where I is the total current flowing from the source. Often a current dipole is defined as a source and a sink of current very close to each other and with the same magnitude.

Radial and Non-Radial Current Dipoles

The first basic problem to solve is that of a radial current dipole. From the electromagnetic point of view we must solve the Poisson's Equation in an inhomogeneous medium. (We start with a current dipole rather than a simple current source, because we assumed that the surrounding medium has a zero conductivity and thus the current flow has to "close" to a sink in a region of interest. In other words in our quasi-static analysis we have to put a source and a sink of the same magnitude in order to "close the circuit", and avoid a (time dependent) accumulation of electric charge at the interface between conducting and non-conducting (outside) media.) Mathematically, we can still find a solution for a source and one for a sink, and then superimpose them before we impose that the conductivity of the surrounding medium is equal to zero. Let's now define the geometry of the problem:
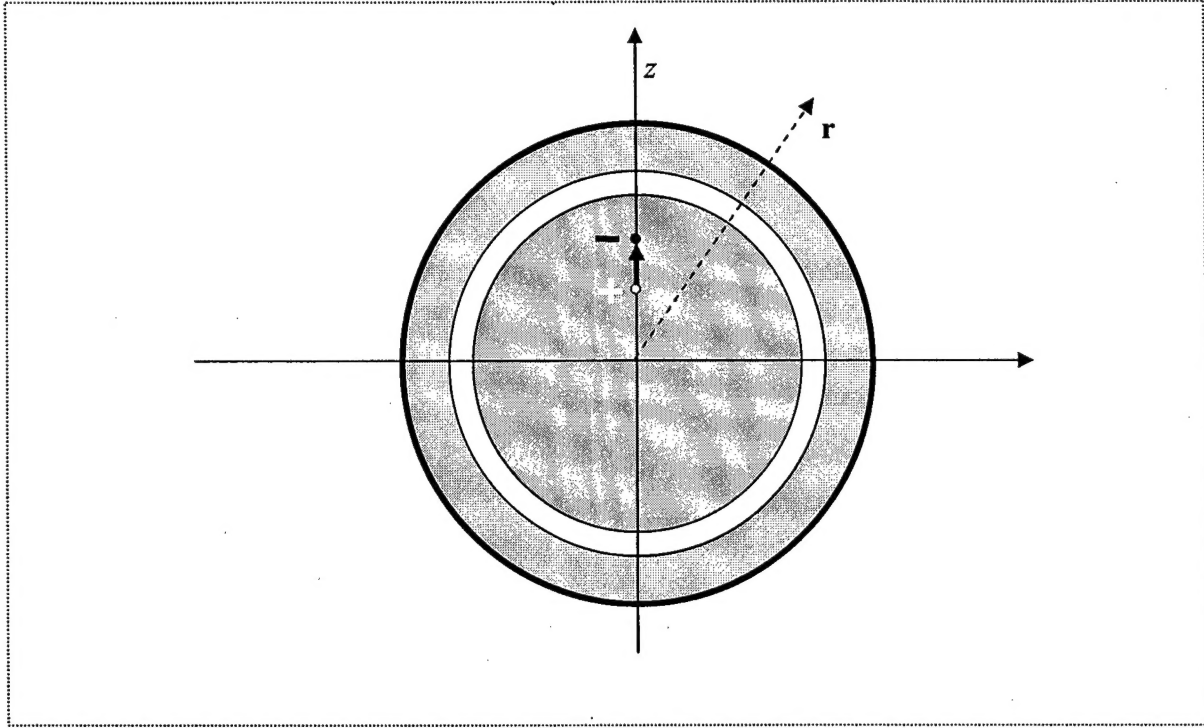
Figure 2. A radial current dipole in the three-shell model

We will use the following names for the different regions:

- Region 1 (Brain): $r < R_1$, conductivity σ_1
- Region 2 (Skull): $R_1 \leq r < R_2$, conductivity σ_2
- Region 3 (Scalp): $R_2 \leq r < R_3$, conductivity σ_3
- Region 4 (Free Space): $r > R_3$, conductivity $\sigma_4 = 0$

For the current dipole we assume the following parameters:

- Source Position $r = r_d + \dfrac{d}{2}$, Source Magnitude I

- Sink Position $r = r_d - \dfrac{d}{2}$, Sink Magnitude I

We need to solve the Poisson's Equation in Region 1 with the source and with the sink, and the Laplace's equation in the other regions. We can express the potential in Region1 as the potential due to the current Source in free space plus potential due to the "scattered" field at the interface:

$$\Psi_1 = \Psi_S + \Psi_{S1} \tag{9}$$

where we put:

$$\Psi_S = \frac{1}{4\pi\sigma_1} \frac{I}{\left| r - \left(r_d + \frac{d}{2} \right) \right|} \qquad (10)$$

Because of the azimuthal symmetry of the problem the other term, which is a solution of the homogeneous equation, is:

$$\Psi_{S1} = \sum_{n=0}^{\infty} (a_{1n} r^n + b_{1n} r^{-n-1}) P_n(\cos\theta) \qquad (11)$$

Where $P_n(\cos\theta)$ is the Legendre Polynomial of degree n. In order the potential to be finite it should be:

$$b_{1n} = 0 \qquad (12)$$

In Region 2 we have:

$$\Psi_{S2} = \sum_{n=0}^{\infty} (a_{2n} r^n + b_{2n} r^{-n-1}) P_n(\cos\theta) \qquad (13)$$

In Region 3 we have:

$$\Psi_{S3} = \sum_{n=0}^{\infty} (a_{3n} r^n + b_{3n} r^{-n-1}) P_n(\cos\theta) \qquad (14)$$

and finally in Region 4:

$$\Psi_{S4} = \sum_{n=0}^{\infty} (a_{4n} r^n + b_{4n} r^{-n-1}) P_n(\cos\theta) \qquad (15)$$

But in order the potential to vanish at infinity it must be:

$$a_{4n} = 0 \qquad (16)$$

In order to impose the boundary conditions, we can expand the potential (10) due to the Current Source using the orthogonality properties of the Legendre Polynomials, as follows:

$$\Psi_S = \frac{1}{4\pi\sigma_1} \frac{I}{\left| r - \left(r_d + \frac{d}{2} \right) \right|} = \frac{I}{4\pi\sigma_1} \sum_{n=0}^{\infty} \frac{\left(\min\left[r, \left(r_d + \frac{d}{2} \right) \right] \right)^n}{\left(\max\left[r, \left(r_d + \frac{d}{2} \right) \right] \right)^{n+1}} P_n(\cos\theta) \qquad (17)$$

Now we impose the boundary conditions at each interface. At the first interface we have:

$$\begin{cases} \Psi_S(R_1) + \Psi_{S1}(R_1) = \Psi_{S2}(R_1) \\ \sigma_1 \left.\dfrac{\partial \Psi_S(r)}{\partial r}\right|_{R_1} + \sigma_1 \left.\dfrac{\partial \Psi_{S1}(r)}{\partial r}\right|_{R_1} = \sigma_2 \left.\dfrac{\partial \Psi_{S2}(r)}{\partial r}\right|_{R_1} \end{cases} \tag{18}$$

At the second interface:

$$\begin{cases} \Psi_{S2}(R_2) = \Psi_{S3}(R_2) \\ \sigma_2 \left.\dfrac{\partial \Psi_{S2}(r)}{\partial r}\right|_{R_2} = \sigma_3 \left.\dfrac{\partial \Psi_{S3}(r)}{\partial r}\right|_{R_2} \end{cases} \tag{19}$$

And at the third one:

$$\begin{cases} \Psi_{S3}(R_3) = \Psi_{S4}(R_3) \\ \sigma_3 \left.\dfrac{\partial \Psi_{S3}(r)}{\partial r}\right|_{R_3} = \sigma_4 \left.\dfrac{\partial \Psi_{S4}(r)}{\partial r}\right|_{R_3} \end{cases} \tag{20}$$

Based on what we said before we cannot set $\sigma_4 = 0$ yet. (One can show that if we set $\sigma_4 = 0$ at this stage, the linear system has an indeterminate solution. This can be explained as follows: Let's assume that $\sigma_4 = 0$, in this case the second equation in (20)becomes:

$$\sigma_3 \left.\frac{\partial \Psi_{S3}(r)}{\partial r}\right|_{R_3} = 0 \tag{21}$$

So all coefficients other than a_3 are equal to zero, so:

$$\Psi_{S3}(r) = a_3 \tag{22}$$

If we put (22) in (19) we obtain

$$\Psi_{S2}(R_2) = a_3 \tag{23}$$

And finally if we put (23) in (18) we obtain:

$$\begin{cases} \Psi_S(R_1) + \Psi_{S1}(R_1) = a_3 \\ \dfrac{\partial \Psi_S(r)}{\partial r}\bigg|_{R_1} + \dfrac{\partial \Psi_{S1}(r)}{\partial r}\bigg|_{R_1} = 0 \end{cases} \qquad (24)$$

And from (24) we have

$$a_3 - a_1 = \frac{1}{R_1} \qquad (25)$$

and we cannot get a unique solution.)

We can solve the same problem for the negative source and add the result to the one obtained for the positive source. Only at this point we can set $\sigma_4 = 0$ to get the final result for the potential distribution due to the current dipole. In Figure 3 we show the distribution of electric potential due to a radial current dipole. In the figure we can see the equipotential lines. We used the following numerical parameters:

Region 1 (Brain): radius = 7.65 cm $\quad \sigma_1 = \dfrac{1}{350}$

Region 2 (Skull): thickness = 0.8 cm $\quad \sigma_2 = \dfrac{1}{20000} \qquad (26)$

Region 3 (Scalp): thickness = 0.2 cm $\quad \sigma_3 = \dfrac{1}{350}$
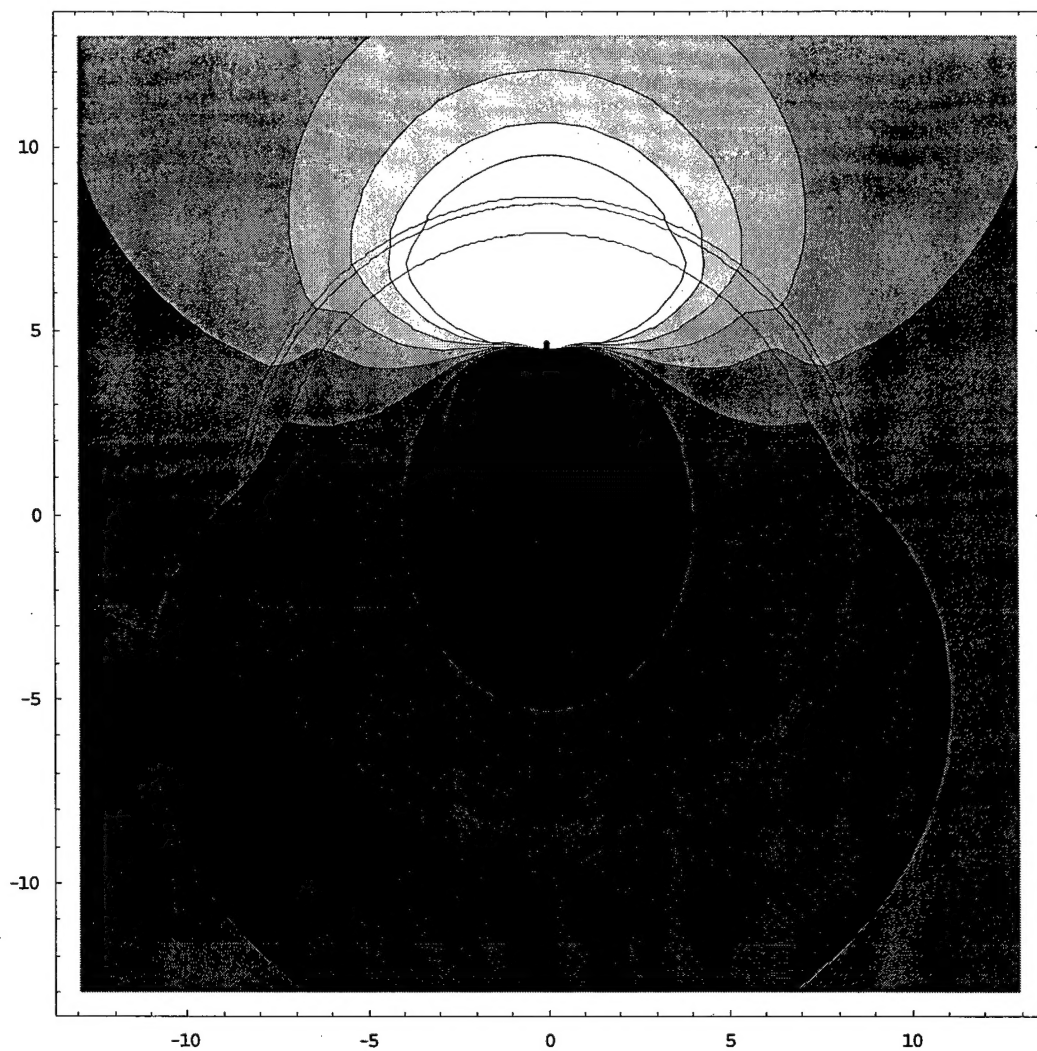
Figure 3. Potential distributions due a current dipole in three-shell model

Using the same technique we can analyze the case depicted in Figure 5 of non radial current dipole.
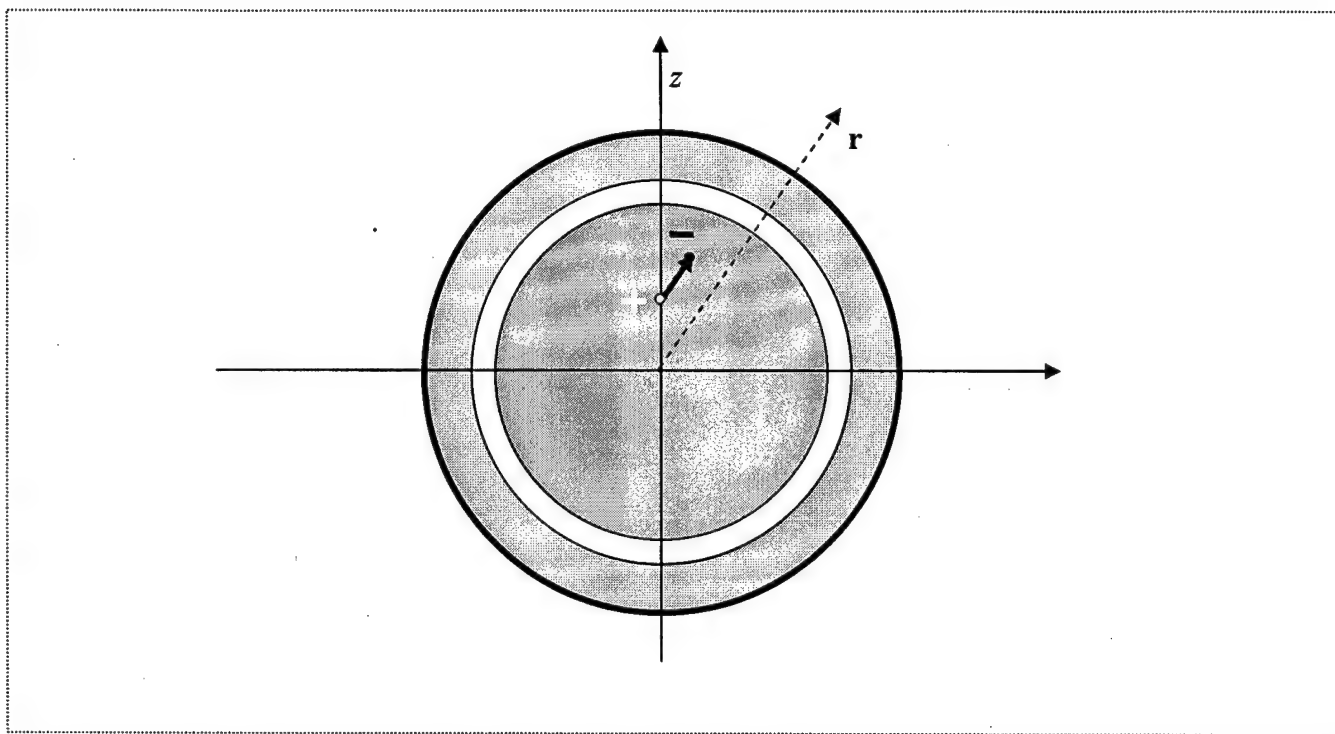

Figure 4: A non-radial current dipole in three-shell model

In this case, we no longer have the azimuthal symmetry of the previous case, but we can still separately calculate the contribution of the positive and the negative source and then we superimpose the effects. The result of this simulation is shown in Figure 5. It is worth highlighting from the Figures 3 and 5 that a distribution of potential could be measured even at a point away (i.e., non-contact) from the scalp surface.
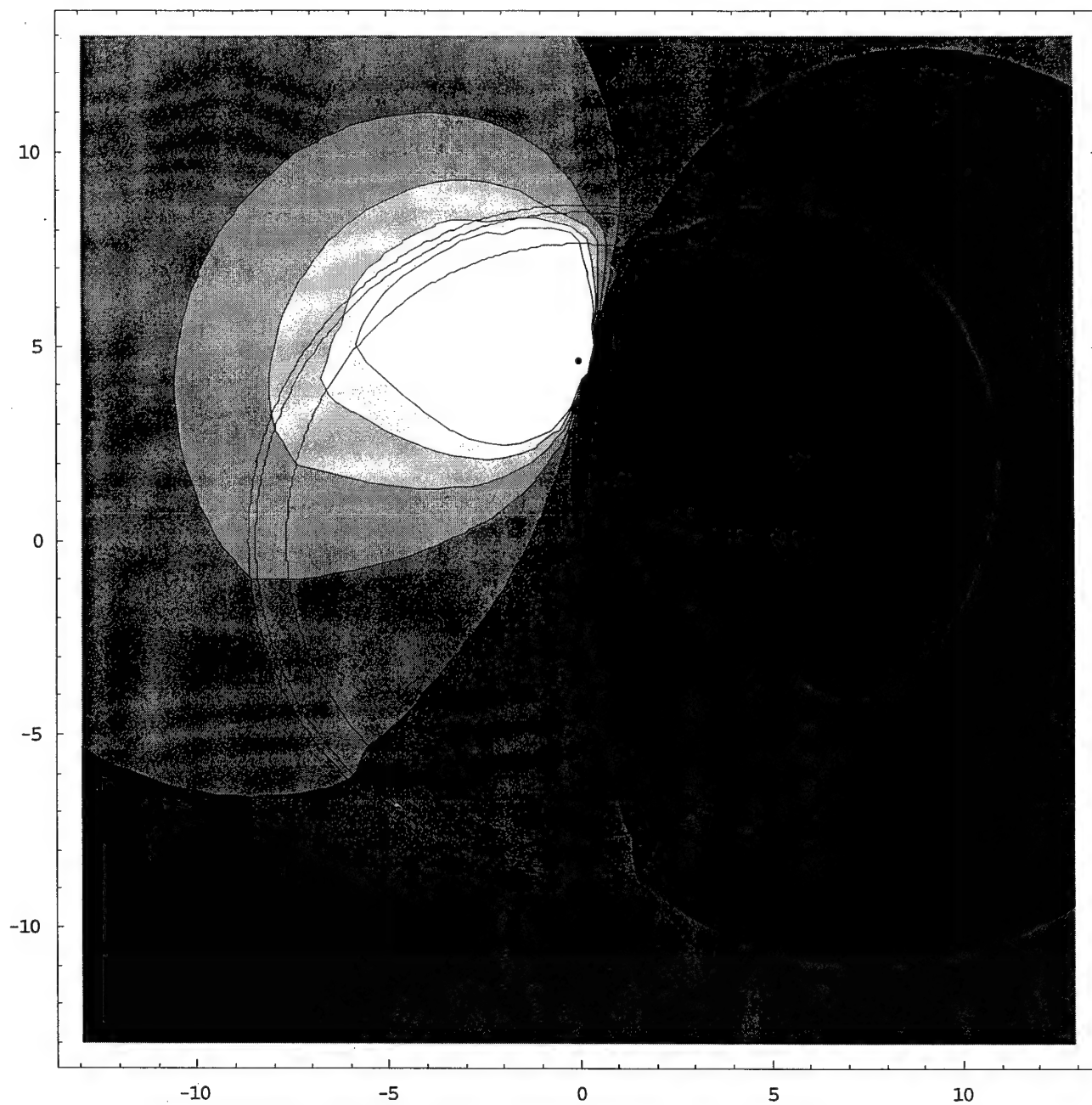
Figure 5: Potential distribution from a non-radial current dipole in three –shell model.

Modeling of a Probe: Perturbed Solution

How is the potential distribution perturbed by the presence of a conductive small probe inside the structure or on the surface? The configuration that we have analyze is shown in Figure 6.
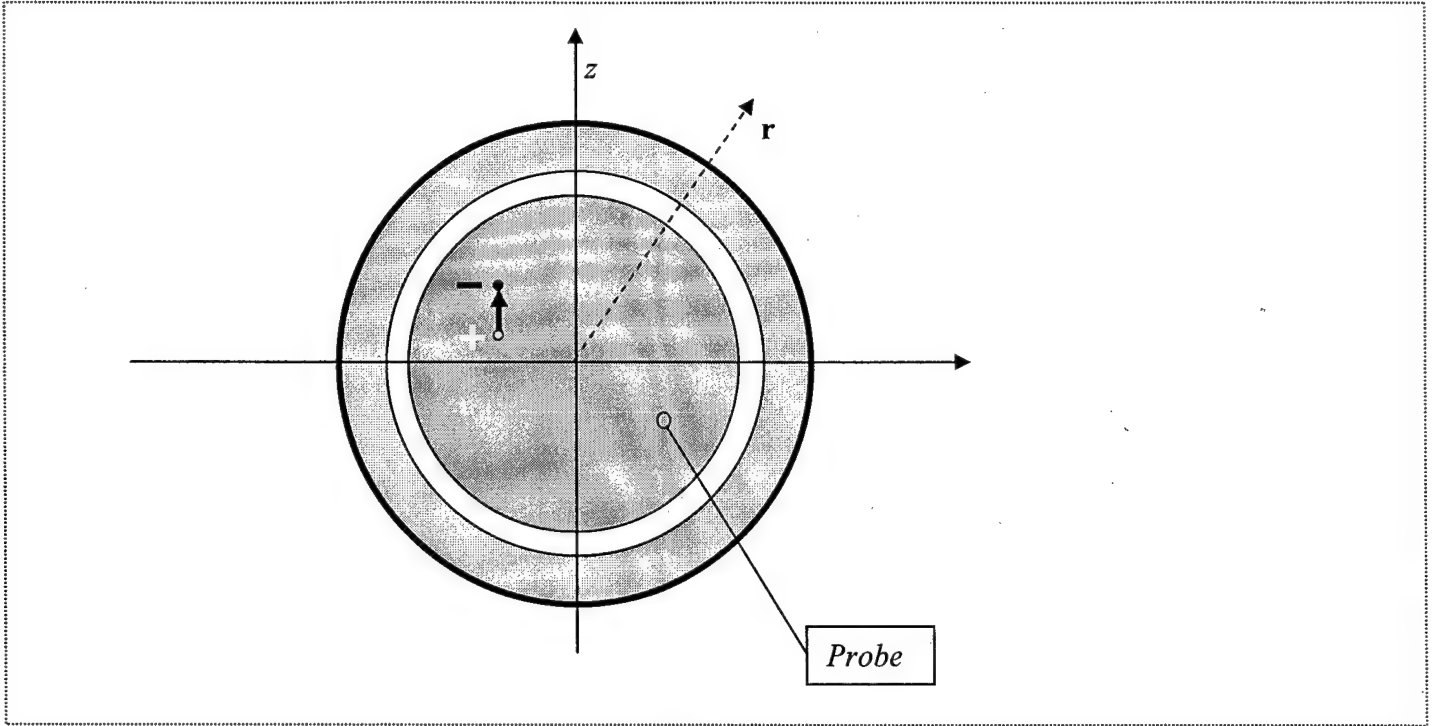

Figure 6

We assume that the radius of the spherical probe is r_p and its conductivity is σ_p. We use the perturbation approach. First, we calculate the potential on the structure without the probe and evaluate the electric field at the point where the probe is to be located. Since the probe is very small we assume that the incident field is "uniform" over the region that is to be occupied by the probe, and is equal to the unperturbed field in the center of the probe. Let's denote the unperturbed potential as $\Psi_0(r,\theta,\varphi)$. The electric field will be:

$$\mathbf{E}_0(r,\theta,\varphi) = -\nabla\Psi_0(r,\theta,\varphi) \tag{27}$$

If the position of the probe is $\{r_0,\theta_0,\varphi_0\}$, the electric field that excites the probe is:

$$\mathbf{E}_0 = \mathbf{E}_0(r_0,\theta_0,\varphi_0) \tag{28}$$

Due to these assumptions, this field induces a uniform field inside the probe, equal to:

$$\mathbf{E}_p = \frac{3\sigma_1}{\sigma_p + 2\sigma_1} \mathbf{E}_0 \tag{29}$$

and its dipole moment is given by:

$$\mathbf{p} = 4\pi\sigma_1 \frac{\sigma_p - \sigma_1}{\sigma_p + 2\sigma_1} r_p^3 \mathbf{E}_0 \tag{30}$$

The presence of the probe alters the distribution of potential by the amount:

$$\Psi_p = \frac{\sigma_p - \sigma_1}{\sigma_p + 2\sigma_1} E_0 \frac{r_p^3}{|\mathbf{r} - \mathbf{r}_0|^2} \cos\gamma \tag{31}$$

The angle γ, shown in Figure 7, is the angle that the vector going from the center of the probe to the observation point forms with the incident electric field on the probe.
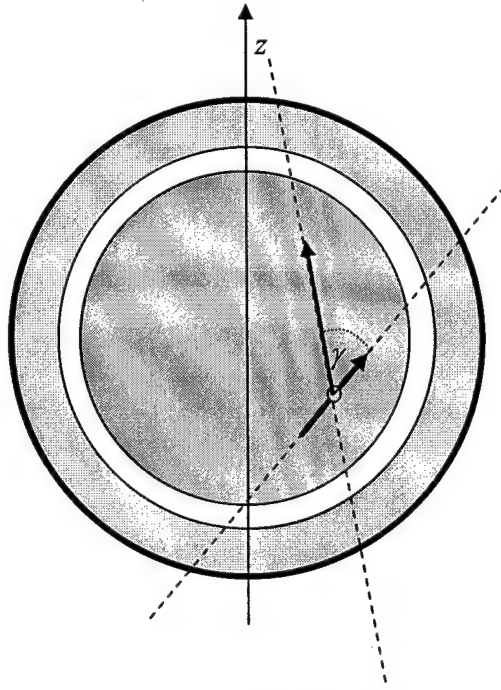

Figure 7

The angle γ can be written as:

$$\cos\gamma = \frac{(\mathbf{r} - \mathbf{r}_0) \cdot \mathbf{E}_0}{|\mathbf{r} - \mathbf{r}_0| E_0} \tag{32}$$

From this, (31) can be expressed as:

$$\Psi_p = \frac{\sigma_p - \sigma_1}{\sigma_p + 2\sigma_1} E_0 \frac{r_p^3}{|\mathbf{r} - \mathbf{r}_0|^2} \frac{(\mathbf{r} - \mathbf{r}_0) \cdot \mathbf{E}_0}{|\mathbf{r} - \mathbf{r}_0| E_0} \tag{33}$$

This is a first-order approximate of the perturbation due to the presence of the probe. This can be further improved as follows: After the introduction of the perturbed field in (33) due to the probe, the boundary conditions are no more satisfied, so we have to solve again the problem of Poisson equation, with the induced dipole on the probe as a secondary source. We will then superimpose the perturbed potential with the unperturbed potential. We assume that the induced dipole on the probe is due to a positive and a negative source of current close to each other in such a way that the induced current dipole is given as:

$$\mathbf{p} = 4\pi\sigma_1 \frac{\sigma_p - \sigma_1}{\sigma_p + 2\sigma_1} r_p^3 \mathbf{E}_0 = 4\pi\sigma_1 I_p \mathbf{L} \tag{34}$$
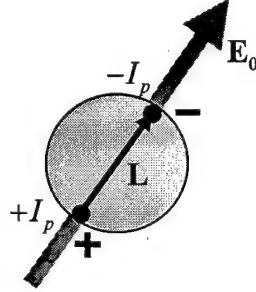
which is:

$$\frac{\sigma_p - \sigma_1}{\sigma_p + 2\sigma_1} r_p^3 \mathbf{E}_0 = I_p \mathbf{L} \tag{35}$$

Our constraint is on the dipole moment, so we have a degree of freedom in choosing I_p and $|\mathbf{L}|$. We arbitrarily choose $|\mathbf{L}|$ to be equal to the diameter of the probe $2r_p$, and then we have:

$$\begin{cases} I_p = \dfrac{\sigma_p - \sigma_1}{\sigma_p + 2\sigma_1} \dfrac{r_p^2}{2} |\mathbf{E}_0| \\ \mathbf{L} = 2r_p \dfrac{\mathbf{E}_0}{|\mathbf{E}_0|} \end{cases} \tag{36}$$

In this way the two sources are given by:

$$\begin{cases} I_{p+}(\mathbf{r}) = I_p \delta\left[\mathbf{r} - \left(\mathbf{r}_0 + r_p \dfrac{\mathbf{E}_0}{|\mathbf{E}_0|}\right)\right] \\[4mm] I_{p-}(\mathbf{r}) = -I_p \delta\left[\mathbf{r} - \left(\mathbf{r}_0 - r_p \dfrac{\mathbf{E}_0}{|\mathbf{E}_0|}\right)\right] \end{cases} \tag{37}$$

As in the unperturbed potential, we can now solve two separate problems with azimuthal symmetry and then superimpose the solutions to have the total perturbation potential. In the Figures 8 and 9, the green "dot" shows the position of the probe.

As we can see, there is almost no change in the potential provided the probe is small.

(2)   Electromagnetic model for the interpretation of the potential distribution over the scalp due to electrical activity inside the brain: Electrodynamic Approach

We can also analyze this structure using the electrodynamical approach. In this case we substitute the current dipole used in the quasi-static analysis by an electromagnetic dipole. From the electromagnetic view point, we have to solve the problem of the radiation by an electric dipole in a multi-layered medium with different finite conductivities.

Tai and Collin in their 2000 paper in the *IEEE Transactions on Antennas and Propagation* (Vol. 48, No. 10, October 2000, pp. 1501-1506)[6] discussed an interesting problem dealing with radiation of a Hertzian dipole in a conducting medium. They concluded that if a dipole is totally immersed in a finitely conductive medium, for a given dipole moment the total radiating power can theoretically be infinite. They mention that this is due to the dissipation of energy in the immediate vicinity of such a dipole where the field can in principle be infinitely strong. Then they analyzed the case of an insulated dipole in a conducting medium, in which the dipole is insulated by a lossless dielectric sphere and then it is immersed in a finitely conducting medium of infinite extent. Their results show that in this case the radiated power is finite. This problem has direct relevance to the EEG problems in which induced dipoles in the brain tissues are effectively dipoles in a conducting medium, resulting in the volume current in this medium. Specifically, it is known that the pyramidal cells, the elongated primary processing neurons of the visual cortex, necessarily act effectively as "current dipoles" because of the spatial distribution of their membrane channels, so that their local "sources" and "sinks" lie at some distance from one another along a line perpendicular to the cortex. Therefore, understanding the behavior of such dipoles in finitely conducting medium is important in the EEG study. Here we have explored the analysis and modeling of fields due to insulated and small dipoles in a conducting sphere of layers with different conductivities: We refer to the geometry in Figure 8 where in general the insulated dipole is off-centered.

---

[6] C. T. Tai and R. E. Collin, "Radiation of a Hertzian Dipole Immersed in a Dissipative Medium," *IEEE Transactions on Antennas and Propagation*, Vol. 48, No. 10, October 2000, pp. 1501-1506
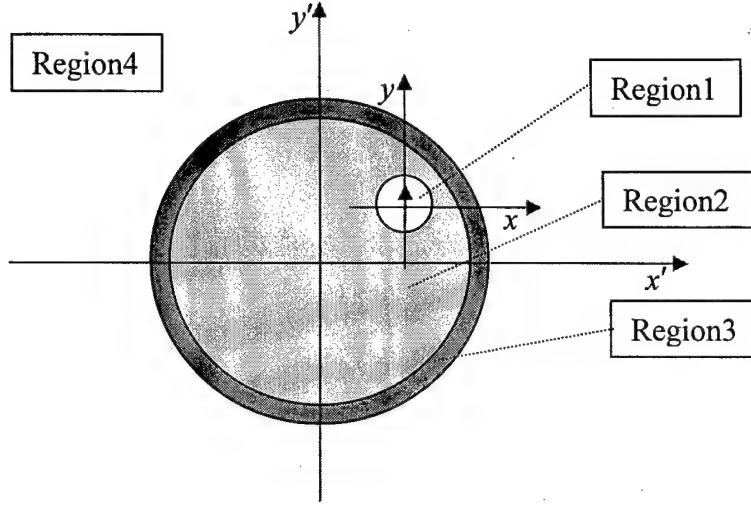
Figure 8. Radiation of a dipole in three-shell model

To solve this problem we expand the electric and the magnetic fields in terms of Spherical Vector Wave Harmonics[7] in each region and with respect to the most convenient reference system between $\{r,\theta,\varphi\}$ and $\{r',\theta',\varphi'\}$. Spherical Vector Wave Harmonics are defined as follows:

$$
\begin{cases}
\mathbf{M}_{n,m}(r,\theta,\varphi) = \nabla u_{n,m}(r,\theta,\varphi) \times \hat{\mathbf{r}} \\[2mm]
\mathbf{N}_{n,m}(r,\theta,\varphi) = \dfrac{1}{k}\nabla \times \mathbf{M}_{n,m}(r,\theta,\varphi) \\[2mm]
u_{n,m}(r,\theta,\varphi) = j_n(kr)P_n^m(\cos\theta)e^{im\varphi}
\end{cases}
\tag{38}
$$

$$
\begin{cases}
\mathbf{M}_{n,m}^{(\alpha)}(r,\theta,\varphi) = \nabla u_{n,m}^{(\alpha)}(r,\theta,\varphi) \times \hat{\mathbf{r}} \\[2mm]
\mathbf{N}_{n,m}^{(\alpha)}(r,\theta,\varphi) = \dfrac{1}{k}\nabla \times \mathbf{M}_{n,m}^{(\alpha)}(r,\theta,\varphi) \\[2mm]
u_{n,m}^{(\alpha)}(r,\theta,\varphi) = h_n^{(\alpha)}(kr)P_n^m(\cos\theta)e^{im\varphi}
\end{cases}
\tag{39}
$$

In region 1 we expand the fields with respect to $\{r,\theta,\varphi\}$:

$$
\mathbf{E}_1(r,\theta,\varphi) = \sum_{n=1}^{\infty}\sum_{m=-n}^{n} P_1(n,m)\mathbf{N}_{n,m}(r,\theta,\varphi) + Q_1(n,m)\mathbf{M}_{n,m}(r,\theta,\varphi)
\tag{40}
$$

$$
\mathbf{H}_1(r,\theta,\varphi) = \frac{j}{\eta_1}\sum_{n=1}^{\infty}\sum_{m=-n}^{n} P_1(n,m)\mathbf{M}_{n,m}(r,\theta,\varphi) + Q_1(n,m)\mathbf{N}_{n,m}(r,\theta,\varphi)
\tag{41}
$$

---

[7] .A. Stratton, "*Electromagnetic Theory*", McGraw-Hill, 1941

Due to the presence of the electric dipole in the region 1 we have to write the fields in the following way:

$$
\begin{aligned}
\mathbf{E}_1(r,\theta,\varphi) =& \, P_1^{(1)}(1,0)\mathbf{N}_{1,0}^{(1)}(r,\theta,\varphi) + P_1^{(2)}(1,0)\mathbf{N}_{1,0}^{(2)}(r,\theta,\varphi) + \\
&+ P_1(1,-1)\mathbf{N}_{1,-1}(r,\theta,\varphi) + P_1(1,1)\mathbf{N}_{1,-1}(r,\theta,\varphi) + \\
&+ \sum_{n=2}^{\infty}\sum_{m=-n}^{n} P_1(n,m)\mathbf{N}_{n,m}(r,\theta,\varphi) + \sum_{n=1}^{\infty}\sum_{m=-n}^{n} Q_1(n,m)\mathbf{M}_{n,m}(r,\theta,\varphi)
\end{aligned}
\tag{42}
$$

$$
\begin{aligned}
\mathbf{H}_1(r,\theta,\varphi) =& \, \frac{j}{\eta_1}\Big[P_1^{(1)}(1,0)\mathbf{M}_{1,0}^{(1)}(r,\theta,\varphi) + P_1^{(2)}(1,0)\mathbf{M}_{1,0}^{(2)}(r,\theta,\varphi)\Big] + \\
&+ \frac{j}{\eta_1}\Big[P_1(1,-1)\mathbf{M}_{1,-1}(r,\theta,\varphi) + P_1(1,1)\mathbf{M}_{1,-1}(r,\theta,\varphi)\Big] + \\
&+ \frac{j}{\eta_1}\sum_{n=2}^{\infty}\sum_{m=-n}^{n} P_1(n,m)\mathbf{M}_{n,m}(r,\theta,\varphi) + \sum_{n=1}^{\infty}\sum_{m=-n}^{n} Q_1(n,m)\mathbf{N}_{n,m}(r,\theta,\varphi)
\end{aligned}
\tag{43}
$$

In region 2 we expand the fields with respect to $\{r,\theta,\varphi\}$:

$$
\begin{aligned}
\mathbf{E}_2(r,\theta,\varphi) =& \sum_{n=1}^{\infty}\sum_{m=-n}^{n} P_2^{(1)}(n,m)\mathbf{N}_{n,m}^{(1)}(r,\theta,\varphi) + Q_2^{(1)}(n,m)\mathbf{M}_{n,m}^{(1)}(r,\theta,\varphi) + \\
&+ \sum_{n=1}^{\infty}\sum_{m=-n}^{n} P_2^{(2)}(n,m)\mathbf{N}_{n,m}^{(2)}(r,\theta,\varphi) + Q_2^{(2)}(n,m)\mathbf{M}_{n,m}^{(2)}(r,\theta,\varphi)
\end{aligned}
\tag{44}
$$

$$
\begin{aligned}
\mathbf{H}_2(r,\theta,\varphi) =& \, \frac{j}{\eta_2}\sum_{n=1}^{\infty}\sum_{m=-n}^{n} P_2^{(1)}(n,m)\mathbf{M}_{n,m}^{(1)}(r,\theta,\varphi) + Q_2^{(1)}(n,m)\mathbf{N}_{n,m}^{(1)}(r,\theta,\varphi) + \\
&+ \frac{j}{\eta_2}\sum_{n=1}^{\infty}\sum_{m=-n}^{n} P_2^{(2)}(n,m)\mathbf{M}_{n,m}^{(2)}(r,\theta,\varphi) + Q_2^{(2)}(n,m)\mathbf{N}_{n,m}^{(2)}(r,\theta,\varphi)
\end{aligned}
\tag{45}
$$

In region 2 we also expand the fields with respect to $\{r',\theta',\varphi'\}$:

$$
\begin{aligned}
\mathbf{E}_2(r',\theta',\varphi') =& \sum_{n=1}^{\infty}\sum_{m=-n}^{n} A_2^{(1)}(n,m)\mathbf{N}_{n,m}^{(1)}(r',\theta',\varphi') + B_2^{(1)}(n,m)\mathbf{M}_{n,m}^{(1)}(r',\theta',\varphi') + \\
&+ \sum_{n=1}^{\infty}\sum_{m=-n}^{n} A_2^{(2)}(n,m)\mathbf{N}_{n,m}^{(2)}(r',\theta',\varphi') + B_2^{(2)}(n,m)\mathbf{M}_{n,m}^{(2)}(r',\theta',\varphi')
\end{aligned}
\tag{46}
$$

$$
\begin{aligned}
\mathbf{H}_2(r',\theta',\varphi') =& \, \frac{j}{\eta_2}\sum_{n=1}^{\infty}\sum_{m=-n}^{n} A_2^{(1)}(n,m)\mathbf{M}_{n,m}^{(1)}(r',\theta',\varphi') + B_2^{(1)}(n,m)\mathbf{N}_{n,m}^{(1)}(r',\theta',\varphi') + \\
&+ \frac{j}{\eta_2}\sum_{n=1}^{\infty}\sum_{m=-n}^{n} A_2^{(2)}(n,m)\mathbf{M}_{n,m}^{(2)}(r',\theta',\varphi') + B_2^{(2)}(n,m)\mathbf{N}_{n,m}^{(2)}(r',\theta',\varphi')
\end{aligned}
\tag{47}
$$

In region 3 and in region 4 we expand the fields with respect to $\{r', \theta', \varphi'\}$:

$$
\begin{aligned}
\mathbf{E}_3(r',\theta',\varphi') &= \sum_{n=1}^{\infty}\sum_{m=-n}^{n} A_3^{(1)}(n,m)\mathbf{N}_{n,m}^{(1)}(r',\theta',\varphi') + B_3^{(1)}(n,m)\mathbf{M}_{n,m}^{(1)}(r',\theta',\varphi') + \\
&+ \sum_{n=1}^{\infty}\sum_{m=-n}^{n} A_3^{(2)}(n,m)\mathbf{N}_{n,m}^{(2)}(r',\theta',\varphi') + B_3^{(2)}(n,m)\mathbf{M}_{n,m}^{(2)}(r',\theta',\varphi')
\end{aligned}
\tag{48}
$$

$$
\begin{aligned}
\mathbf{H}_3(r',\theta',\varphi') &= \frac{j}{\eta_3}\sum_{n=1}^{\infty}\sum_{m=-n}^{n} A_3^{(1)}(n,m)\mathbf{M}_{n,m}^{(1)}(r',\theta',\varphi') + B_3^{(1)}(n,m)\mathbf{N}_{n,m}^{(1)}(r',\theta',\varphi') + \\
&+ \frac{j}{\eta_3}\sum_{n=1}^{\infty}\sum_{m=-n}^{n} A_3^{(2)}(n,m)\mathbf{M}_{n,m}^{(2)}(r',\theta',\varphi') + B_3^{(2)}(n,m)\mathbf{N}_{n,m}^{(2)}(r',\theta',\varphi')
\end{aligned}
\tag{49}
$$

In region 4 we impose also the radiation condition:

$$
\mathbf{E}_4(r',\theta',\varphi') = \sum_{n=1}^{\infty}\sum_{m=-n}^{n} A_4^{(2)}(n,m)\mathbf{N}_{n,m}^{(2)}(r',\theta',\varphi') + B_4^{(2)}(n,m)\mathbf{M}_{n,m}^{(2)}(r',\theta',\varphi')
\tag{50}
$$

$$
\mathbf{H}_4(r',\theta',\varphi') = \frac{j}{\eta_4}\sum_{n=1}^{\infty}\sum_{m=-n}^{n} A_4^{(2)}(n,m)\mathbf{M}_{n,m}^{(2)}(r',\theta',\varphi') + B_4^{(2)}(n,m)\mathbf{N}_{n,m}^{(2)}(r',\theta',\varphi')
\tag{51}
$$

By imposing the boundary conditions, we can find the unknown coefficients. Obviously, we can easily impose the boundary conditions for fields expressed in the same reference system, so we can impose the boundary conditions at the interface between regions 1 and 2 using the reference system $\{r,\theta,\varphi\}$. At the interface between regions 2 and 3, we use the reference system $\{r',\theta',\varphi'\}$. Then we have to impose the Source Condition:

$$
P_1^{(1)}(1,0) + P_1^{(2)}(1,0) = \frac{J}{4\pi}
\tag{52}
$$

Finally we have to relate the field in region 2 expressed in both reference systems by using the addition theorem for spherical vector wave functions.

Let's consider the electric field in the region 2 written in both reference systems:

$$
\begin{cases}
\mathbf{E}_2(r,\theta,\varphi) = \sum_{n=1}^{\infty}\sum_{m=-n}^{n} P_2^{(1)}(n,m)\mathbf{N}_{n,m}^{(1)}(r,\theta,\varphi) + Q_2^{(1)}(n,m)\mathbf{M}_{n,m}^{(1)}(r,\theta,\varphi) + \\
\qquad + \sum_{n=1}^{\infty}\sum_{m=-n}^{n} P_2^{(2)}(n,m)\mathbf{N}_{n,m}^{(2)}(r,\theta,\varphi) + Q_2^{(2)}(n,m)\mathbf{M}_{n,m}^{(2)}(r,\theta,\varphi) \\
\mathbf{E}_2(r',\theta',\varphi') = \sum_{n=1}^{\infty}\sum_{m=-n}^{n} A_2^{(1)}(n,m)\mathbf{N}_{n,m}^{(1)}(r',\theta',\varphi') + B_2^{(1)}(n,m)\mathbf{M}_{n,m}^{(1)}(r',\theta',\varphi') + \\
\qquad + \sum_{n=1}^{\infty}\sum_{m=-n}^{n} A_2^{(2)}(n,m)\mathbf{N}_{n,m}^{(2)}(r',\theta',\varphi') + B_2^{(2)}(n,m)\mathbf{M}_{n,m}^{(2)}(r',\theta',\varphi')
\end{cases}
\tag{53}
$$

The Addition Theorem for the spherical vector wave functions[8] states:

$$
\begin{cases}
\mathbf{N}_{n,m}^{(\alpha)}(r,\theta,\varphi) = \sum_{\nu=1}^{\infty} \sum_{\mu=-\nu}^{\nu} X^{(\alpha)}(n,m,\nu,\mu)\mathbf{N}_{\nu,\mu}^{(\alpha)}(r',\theta',\varphi') + Y^{(\alpha)}(n,m,\nu,\mu)\mathbf{M}_{\nu,\mu}^{(\alpha)}(r',\theta',\varphi') \\
\mathbf{M}_{n,m}^{(\alpha)}(r,\theta,\varphi) = \sum_{\nu=1}^{\infty} \sum_{\mu=-\nu}^{\nu} X^{(\alpha)}(n,m,\nu,\mu)\mathbf{M}_{\nu,\mu}^{(\alpha)}(r',\theta',\varphi') + Y^{(\alpha)}(n,m,\nu,\mu)\mathbf{N}_{\nu,\mu}^{(\alpha)}(r',\theta',\varphi')
\end{cases}
\tag{54}
$$

where:

$$
\begin{cases}
X^{(\alpha)}(n,m,\nu,\mu) = (-1)^{\mu}\sum_{p} a(m,n|-\mu,\nu|p,p)c(n,\nu,p)h_{p}^{(\alpha)}(kr_0)P_{p}^{m-\mu}(\cos\theta_0)e^{i(m-\mu)\varphi_0} \\[2mm]
y^{(\alpha)}(n,m,\nu,\mu) = (-1)^{\mu+1}\sum_{p} a(m,n|-\mu,\nu|p,p-1)d(n,\nu,p)h_{p}^{(\alpha)}(kr_0)P_{p}^{m-\mu}(\cos\theta_0)e^{i(m-\mu)\varphi_0} \\[2mm]
c(n,\nu,p) = i^{\nu+p-n}\dfrac{[2\nu(\nu+1)(2\nu+1)+(\nu+1)(n-\nu+p+1)(n+\nu-p)-\nu(\nu-n+p+1)(n+\nu+p+2)]}{2\nu(\nu+1)} \\[4mm]
d(n,\nu,p) = i^{\nu+p-n}\dfrac{(2\nu+1)\sqrt{(n+\nu+p+1)(\nu-n+p)(n-\nu+p)(n+\nu-p+1)}}{2\nu(\nu+1)}
\end{cases}
\tag{55}
$$

Using that theorem we can write the field in region 2 as:
$$\mathbf{E}_2(r,\theta,\varphi) \to \mathbf{E}_2(r',\theta',\varphi') =$$

$$
\begin{aligned}
&= \sum_{n=1}^{\infty}\sum_{m=-n}^{n} P_2^{(1)}(n,m)\left(\sum_{\nu=1}^{\infty}\sum_{\mu=-\nu}^{\nu} X^{(1)}(n,m,\nu,\mu)\mathbf{N}_{\nu,\mu}^{(1)}(r',\theta',\varphi') + X^{(1)}(n,m,\nu,\mu)\mathbf{M}_{\nu,\mu}^{(1)}(r',\theta',\varphi')\right) + \\
&+ \sum_{n=1}^{\infty}\sum_{m=-n}^{n} Q_2^{(1)}(n,m)\left(\sum_{\nu=1}^{\infty}\sum_{\mu=-\nu}^{\nu} X^{(1)}(n,m,\nu,\mu)\mathbf{M}_{\nu,\mu}^{(1)}(r',\theta',\varphi') + X^{(1)}(n,m,\nu,\mu)\mathbf{N}_{\nu,\mu}^{(1)}(r',\theta',\varphi')\right) + \\
&+ \sum_{n=1}^{\infty}\sum_{m=-n}^{n} P_2^{(2)}(n,m)\left(\sum_{\nu=1}^{\infty}\sum_{\mu=-\nu}^{\nu} X^{(2)}(n,m,\nu,\mu)\mathbf{N}_{\nu,\mu}^{(2)}(r',\theta',\varphi') + X^{(2)}(n,m,\nu,\mu)\mathbf{M}_{\nu,\mu}^{(2)}(r',\theta',\varphi')\right) + \\
&+ \sum_{n=1}^{\infty}\sum_{m=-n}^{n} Q_2^{(2)}(n,m)\left(\sum_{\nu=1}^{\infty}\sum_{\mu=-\nu}^{\nu} X^{(2)}(n,m,\nu,\mu)\mathbf{M}_{\nu,\mu}^{(2)}(r',\theta',\varphi') + X^{(2)}(n,m,\nu,\mu)\mathbf{N}_{\nu,\mu}^{(2)}(r',\theta',\varphi')\right)
\end{aligned}
\tag{56}
$$

At this point we change the order of the summations in (56) and we obtain:

[8] O.R. Cruzan, "*Translational Addition Theorems for Spherical Vector Wave Functions*", Q. Appl. Math., vol. 20, pp 33-40, 1962

$$\mathbf{E}_2(r',\theta',\varphi') =$$

$$= \sum_{\nu=1}^{\infty} \sum_{\mu=-\nu}^{\nu} \left[\sum_{n=1}^{\infty} \sum_{n=-n}^{n} P_2^{(1)}(n,m) X^{(1)}(n,m,\nu,\mu) + Q_2^{(1)}(n,m) Y^{(1)}(n,m,\nu,\mu) \right] \mathbf{N}_{\nu,\mu}^{(1)}(r',\theta',\varphi') +$$

$$+ \sum_{\nu=1}^{\infty} \sum_{\mu=-\nu}^{\nu} \left[\sum_{n=1}^{\infty} \sum_{m=-n}^{n} P_2^{(1)}(n,m) Y^{(1)}(n,m,\nu,\mu) + Q_2^{(1)}(n,m) X^{(1)}(n,m,\nu,\mu) \right] \mathbf{M}_{\nu,\mu}^{(1)}(r',\theta',\varphi') +$$

$$\sum_{\nu=1}^{\infty} \sum_{\mu=-\nu}^{\nu} \left[\sum_{n=1}^{\infty} \sum_{n=-n}^{n} P_2^{(2)}(n,m) X^{(2)}(n,m,\nu,\mu) + Q_2^{(2)}(n,m) Y^{(2)}(n,m,\nu,\mu) \right] \mathbf{N}_{\nu,\mu}^{(2)}(r',\theta',\varphi') +$$

$$+ \sum_{\nu=1}^{\infty} \sum_{\mu=-\nu}^{\nu} \left[\sum_{n=1}^{\infty} \sum_{m=-n}^{n} P_2^{(2)}(n,m) Y^{(2)}(n,m,\nu,\mu) + Q_2^{(2)}(n,m) X^{(2)}(n,m,\nu,\mu) \right] \mathbf{M}_{\nu,\mu}^{(2)}(r',\theta',\varphi')$$

$$(57)$$

At this point we can compare (53) with (57) and we obtain the following relations between coefficients:

$$\begin{cases} A_2^{(1)}(\nu,\mu) = \sum_{n=1}^{\infty} \sum_{n=-n}^{n} P_2^{(1)}(n,m) X^{(1)}(n,m,\nu,\mu) + Q_2^{(1)}(n,m) Y^{(1)}(n,m,\nu,\mu) \\ B_2^{(1)}(\nu,\mu) = \sum_{n=1}^{\infty} \sum_{m=-n}^{n} P_2^{(1)}(n,m) Y^{(1)}(n,m,\nu,\mu) + Q_2^{(1)}(n,m) X^{(1)}(n,m,\nu,\mu) \\ A_2^{(2)}(\nu,\mu) = \sum_{n=1}^{\infty} \sum_{n=-n}^{n} P_2^{(2)}(n,m) X^{(2)}(n,m,\nu,\mu) + Q_2^{(2)}(n,m) Y^{(2)}(n,m,\nu,\mu) \\ B_2^{(2)}(\nu,\mu) = \sum_{n=1}^{\infty} \sum_{m=-n}^{n} P_2^{(2)}(n,m) Y^{(2)}(n,m,\nu,\mu) + Q_2^{(2)}(n,m) X^{(2)}(n,m,\nu,\mu) \end{cases}$$

$$(58)$$

Finally using the conditions (58) we can find all of the unknown coefficients.
It is important to mention that when we impose the boundary conditions at the interfaces 1-2 and 2-3, because of the orthogonality properties of the spherical vector wave functions, we see that all of the equations are decoupled, so we can find immediately a solution. The only equations we have to solve are the conditions (58). In other words the real number of unknowns depends only on the regions with non concentric boundaries, in our case the region 2.

The geometry becomes much simplified if the insulated dipole is located at center of the sphere[9], as shown in Figure 9

---

[9] C.T. Tai, R.E. Collin, "Radiation of a Hertzian Dipole Immersed in a Dissipative Medium", IEEE Trans. Antennas and Propagation, vol. 48, n. 10, October 2000
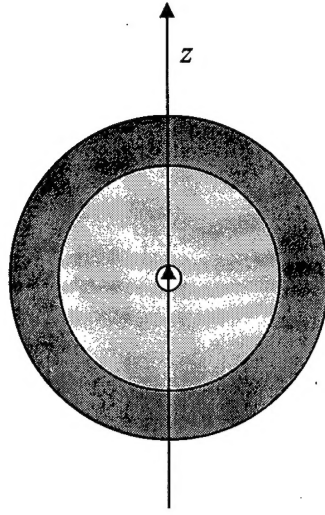
Figure 9

In this case we have 3 concentric dielectric spheres with an electric dipole located in the center. In order to find electric and magnetic fields everywhere we write the Helmholtz's equation for the magnetic vector potential in the four regions:

$$\nabla^2 A_{1z}(\mathbf{r}) + k_1^2 A_{1z}(\mathbf{r}) = -\mu J \delta(\mathbf{r}) \qquad r < r_1 \tag{59}$$

$$\nabla^2 A_{2z}(\mathbf{r}) + k_2^2 A_{2z}(\mathbf{r}) = 0 \qquad r_1 < r < r_2 \tag{60}$$

$$\nabla^2 A_{3z}(\mathbf{r}) + k_3^2 A_{3z}(\mathbf{r}) = 0 \qquad r_2 < r < r_3 \tag{61}$$

$$\nabla^2 A_{4z}(\mathbf{r}) + k_4^2 A_{4z}(\mathbf{r}) = 0 \qquad r > r_3 \tag{62}$$

Due to symmetry, the solutions are written as:

$$\mathbf{A}_i = \left(a_i \frac{e^{-jk_i r}}{r} + b_i \frac{e^{jk_i r}}{r} \right) \hat{\mathbf{z}} \tag{63}$$

$$i = 1, 2, 3, 4$$

In order to find 8 unknown coefficients, we have to impose boundary conditions at each interface (6 equations), the radiation condition (1 equation) and the source condition (1 equation).

The radiation condition states that in the unbounded region, for time-dependence $e^{j\omega t}$, we get :

$$b_4 = 0 \tag{64}$$

For the source condition we consider the inhomogeneous Helmholtz's equation (59) and we integrate both sides in the volume V of a sphere of radius $\alpha \to 0$:

$$\int_V \nabla \cdot \nabla A_{1z}(\mathbf{r}) d\mathbf{r} + k_1^2 \int_V A_{1z}(\mathbf{r}) d\mathbf{r} = -\mu J \qquad r < r_1 \qquad (65)$$

The second integral in the left side is equal to zero for $\alpha \to 0$. We apply the divergence theorem:

$$\int_0^{2\pi} \int_0^\pi \frac{\partial A_{1z}(r,\theta,\varphi)}{\partial r}\bigg|_{r=\alpha} \alpha^2 \sin\theta d\theta d\varphi = -\mu J \qquad r < r_1 \qquad (66)$$

Then we put (63) into (66) and we obtain the source condition:

$$a_1 + b_1 = \frac{\mu J}{4\pi} \qquad (67)$$

For the other boundary conditions we have to calculate electric and magnetic fields in each region:

$$\mathbf{H}_i = \frac{1}{\mu} \nabla \times \mathbf{A}_i \qquad (68)$$

$$\mathbf{E}_i = \frac{\nabla(\nabla \cdot \mathbf{A}_i)}{j\omega\mu\varepsilon_i} - j\omega \mathbf{A}_i \qquad (69)$$

And then we can impose the boundary conditions:

$$\hat{\mathbf{r}} \times \mathbf{E}_1\big|_{r_1} = \hat{\mathbf{r}} \times \mathbf{E}_2\big|_{r_1}$$
$$\hat{\mathbf{r}} \times \mathbf{H}_1\big|_{r_1} = \hat{\mathbf{r}} \times \mathbf{H}_2\big|_{r_1} \qquad (70)$$

$$\hat{\mathbf{r}} \times \mathbf{E}_2\big|_{r_2} = \hat{\mathbf{r}} \times \mathbf{E}_3\big|_{r_2}$$
$$\hat{\mathbf{r}} \times \mathbf{H}_2\big|_{r_2} = \hat{\mathbf{r}} \times \mathbf{H}_3\big|_{r_2} \qquad (71)$$

$$\hat{\mathbf{r}} \times \mathbf{E}_3\big|_{r_3} = \hat{\mathbf{r}} \times \mathbf{E}_4\big|_{r_3}$$
$$\hat{\mathbf{r}} \times \mathbf{H}_3\big|_{r_3} = \hat{\mathbf{r}} \times \mathbf{H}_4\big|_{r_3} \qquad (72)$$

We have to solve the system of equations given by (64), (67), (71) and (72). Once we have the solution of the system we can plot the behavior of the fields. In figure 10, we show the behavior of the absolute value of the transverse electric field.

Transverse Electric Field, $\square\square\square$ 2, Dipole Strenght $\square$ 1
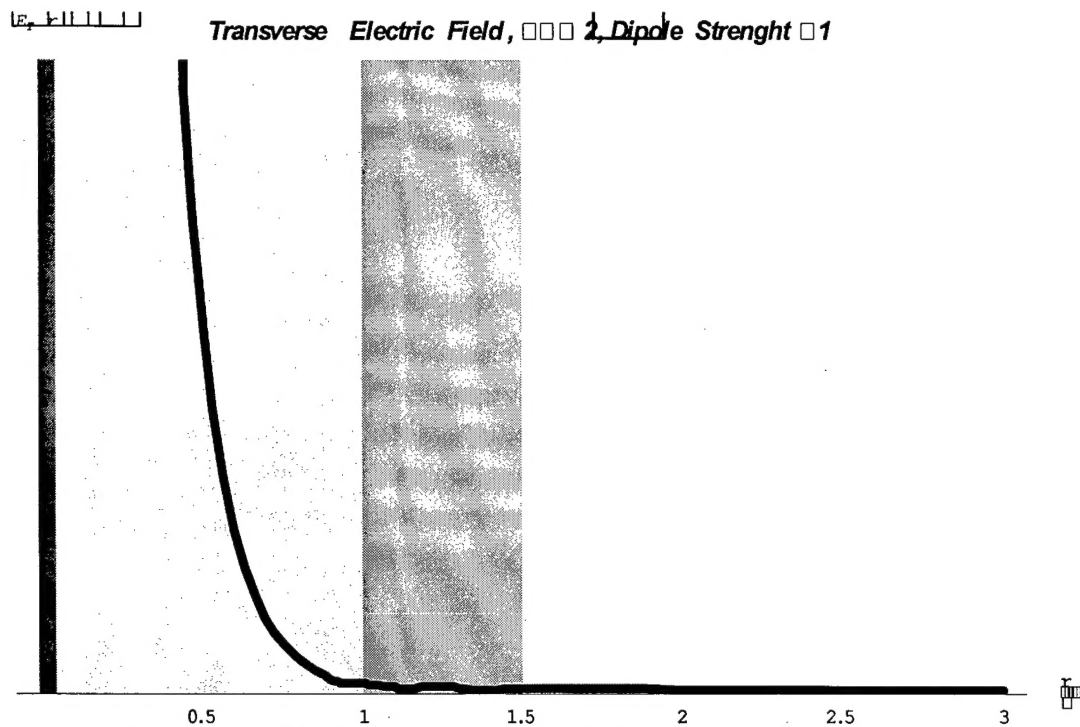
Figure 13. Magnitude of the Transverse electric field of the insulated dipole in finite-radius sphere

In Figure 11, we show Poynting Vector (multiplied by r^2), i.e., the power radiated per unit solid angle, in order to see the effect of dissipation due to the loss:
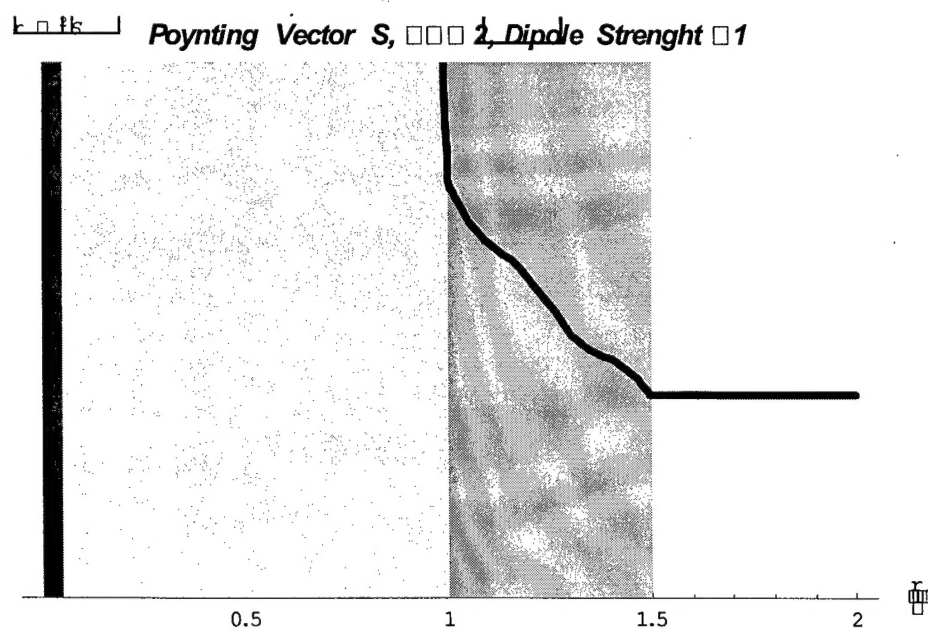
Poynting Vector S, $\square\square\square$ 2, Dipole Strenght $\square$ 1

Figure 14

In the outer region, without loss, the function is constant, as expected.

(3) Potential of a Small Dipole in a Dissipative Medium with Certain Inhomogeneous Conductivity

In our previous study[10], we found that the sagittal fissure in the brain can act as a "major shunt" for electrical current flow, providing evidence that the commonly used 3-sheel model of conductivity may not be adequate in certain conditions. This is due to the fact that the conductivity in the region of sagittal fissure, which is filled with the cerebrospinal fluid (CSF), is different from that of the other inner parts of the brain. In that work, it was shown that a pair of visually-evoked induced "dipole currents", i.e., excited neurons in the visual cortex, oriented ~180 degrees opposite and located across the sagittal fissure produce the scalp potential distributions nearly identical in amplitude and phase, whereas the 3-shell model suggested a mirror-image symmetry across the midline for this potential distribution. Furthermore, the scalp potential around the region of projection of the sagittal fissure onto the scalp had maximum amplitude, which is again different from what the 3-shell model predicted. Here we have explored this issue theoretically by analyzing certain electromagnetic model of a current dipole in a medium with certain inhomogeneous conductivity. We have studied theoretically the potential distribution of a current dipole in a conducting medium with uniform conductivity everywhere, except in a wedge (or a cone) region having a different conductivity (Fig. 12), essentially modeling sagittal fissure shunt. The current dipole can be located at some arbitrary point. We utilized a quasi-static model for this problem and have expressed the electric potentials everywhere.
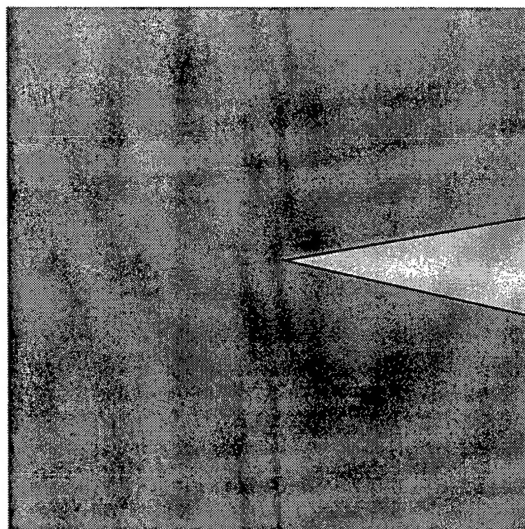

Figure 15. A wedge with a different conductivity that its surrounding region

---

[10] E. N. Pugh, Jr., J. B. Demb, B. Alterman, C. Daniele, L. Daniele, H. Baseler, N. Engheta, and B. Wandell, "Visual potentials evoked by small oscillating sources located by fMRI: the sagittal fissure is a major shunt," a poster presented in the *29th Annual Meeting of the Society for Neuroscience*, in Miami Beach, Florida, October 23-28, 1999.